A Facile Method to Produce Silver Nanoparticle-Loaded Regenerated Cellulose Membranes *via* the Reduction of Silver Nitrate in a Homogeneous System

Yongjian Xu,[a,b,]* Shasha Li,[a,]* and Ping Chang [c]

Regenerated cellulose (RC) membranes loaded with silver nanoparticles (AgNPs) were prepared in this study. Cellulose acted as a reducing agent, silver nitrate acted as an oxidizing agent, and N-methylmorpholine-N-oxide (NMMO) acted as a direct cellulose solvent. The AgNP-loaded RC membranes were obtained *via* the redox reaction between cellulose and silver nitrate. The results of scanning electron microscopy (SEM) and energy dispersive spectroscopy (EDS) analysis suggest that AgNPs were reduced on the RC membranes during the dissolution and regeneration of cellulose. Atomic force microscopy (AFM) showed that the RC membranes exhibited high surface roughness, with a value of 7.19 nm. The Fourier transform infrared spectroscopy (FT-IR) and X-ray diffraction (XRD) results demonstrated that the crystal lattice type of RC membranes changed from cellulose I to cellulose II, without any derivatization. The detection results of atomic absorption spectrometry (AAS) indicated that the silver content of the RC membranes increased with increasing silver nitrate solution concentration. Antibacterial experiments showed that the AgNP-loaded RC membranes exhibited good antibacterial properties with respect to both *Escherichia coli* and *Staphylococcus aureus*.

Keywords: Cellulose antibacterial material; Regenerated cellulose; Cellulose membrane; Silver nano-composites; Antibacterial property

Contact information: a: Shaanxi Key Laboratory on Paper Technology and Specialty Papers, National Demonstration Center for Experimental Light Chemistry Engineering Education, Shaanxi University of Science and Technology, Xi'an, Shaanxi 710021, China; b: State Key Laboratory of Pulp and Paper Engineering, South China University of Technology, Guangzhou, Guangdong 510640, China; c: College of Chemistry and Chemical Engineering, Xi'an Shiyou University, Xi'an, Shaanxi 710021, China;
** Corresponding authors: xuyongjian@sust.edu.cn; 15029292262@163.com*

INTRODUCTION

Nano-sized metal particles have attracted considerable interest (Emam *et al.* 2017a; Emam *et al.* 2017b; Emam *et al.* 2017c). Among the noble nanoparticles, silver nanoparticles (AgNPs) have become the research focus as an antibacterial nanomaterial for biomedical products such as medical devices and wound dressings (Rai *et al.* 2009; Wong and Liu 2010). The antibacterial ability of AgNPs has been exhibited *via* the slow release of silver ions after the AgNPs are attached to microorganisms (Feng *et al.* 2000; Morones *et al.* 2005; Castellano *et al.* 2007). A suitable substrate is indispensable for applying AgNPs in fields such as biomedicine, food, separation technology, and biology. For example, Emam *et al.* (2014) obtained AgNPs using three different cellulosic fibers, *i.e.*, viscose, lyocell and cotton fibers, as the substrates. Among the numerous substrates, regenerated cellulose (RC) has caught the attention of researchers and industry because of its inexpensive, biocompatible, and biodegradable properties (Simmons *et al.* 2011).

Moreover, it can exist in the form of fibers, films, sponges, membranes, and gels, *etc.*, which is beneficial for the incorporation of AgNPs (Fink *et al.* 2001; Luo and Zhang 2013; Kowaluk 2014). RC produced by the N-methylmorpholine-N-oxide (NMMO) method has been industrialized (Lyocell process). NMMO is used as a direct cellulose solvent that can protect the molecular structure of cellulose from destruction (Dogan and Hilmioglu 2009).

Therefore, a method is needed to realize the highly favorable combination of silver and RC materials. Various methods have been reported. In general, they can be divided into the physical adsorption method and the *in-situ* chemical reduction method. In the physical method, a nanosilver collosol (NSC) needs to be fabricated first. Afterward, the NSC is added to a cellulose solution, and the mixture is later regenerated (Chook *et al.* 2014). Alternatively, AgNPs-RC composites can be produced by soaking a prepared RC membrane in the NSC (Ahamed *et al.* 2015). However, the cellulose is merely used as a template during the above procedures. The bonding effects between NSC and RC are relatively weak.

Cellulose, which possesses natural reducing ability, can be employed as a reducing agent. The chemical method can take full advantage of this performance. Wang *et al.* (2014) prepared cellulose hydrogels containing Ag nanoparticles by immersing a RC hydrogel in silver nitrate aqueous solution at 80 °C for 24 h. Nevertheless, the reaction took place in a heterogeneous system, and the reduced AgNPs were simply absorbed on the surface of the RC hydrogel. Thus, the antibacterial ability of the RC hydrogel was somewhat limited. There is therefore an apparent opportunity for RC membranes to be fabricated by reducing silver nitrate in a homogeneous system with cellulose as the sole reducing agent.

In this work, RC antibacterial membranes loaded with AgNPs were prepared *via* the chemical method. Silver nitrate aqueous solution was added to cellulose-NMMO solution, and the redox reaction occurred under homogeneous conditions, in an attempt to uniformly disperse the reduced AgNPs on the subsequent RC membranes. The possible reaction mechanism is shown in Scheme 1. The morphology and surface roughness of RC membranes were investigated, and the variation of the structure and crystal lattice type before and after cellulose regeneration was determined. Furthermore, the antibacterial properties of cellulose membranes containing AgNPs were examined.

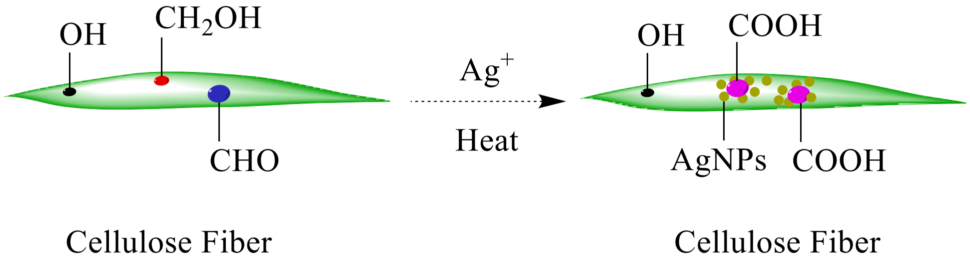

Scheme 1. The reaction mechanism between cellulose and silver

EXPERIMENTAL

Materials

Cotton dissolving pulp fibers (average polymerization degree of 476; α-cellulose content 95%) were kindly provided by Shandong Silver Hawk Co., Ltd, China. The N-methylmorpholine oxide (NMMO·H_2O) (98 + %) was purchased from Alfa Aesar Chemical Co., Ltd, China. Silver nitrate (AR) was purchased from Shanghai Chemical Reagent Co., Ltd, China. Concentrated nitric acid (65% to 68%) was delivered by Sichuan Longxi Chemical Co., Ltd, China. *S. aureus* (ATCC 25923) and *E. coli* (ATCC 8099) were purchased from Nanjing Clinical Biological Technology Co., Ltd, China. Propyl gallate, purchased from Wenzhou Ouhai Chemical Reagent Co., Ltd, China, was used as an antioxidant to avoid oxidation and degradation during the dissolution of cellulose. All chemicals were used without further purification. Deionized water was used in all experiments.

Methods

Preparation of RC membranes

Cotton pulp fibers were smashed by a blender before use. Then, 3 wt% of cellulose solution was prepared as per the following procedures. A set amount of NMMO·H_2O, oven-dried cotton fibers and antioxidant were placed in a round-bottom flask. Then, the flask was heated in a water bath at 90 °C. After the cotton fibers had swelled completely, an agitator was employed until a uniform white solution was obtained. Afterward, silver nitrate solution (0.1 M) with different volume was added. The final silver nitrate percentage in the system was 0.055 wt%, 0.110 wt%, and 0.165 wt%, respectively. Finally, a transparent and amber solution was obtained. Subsequently, the cellulose solution was poured on a plate glass, and then a glass rod was used to scrape the solution into a flat membrane. The plate glass and cellulose solution were then quickly placed into deionized water. After a while, the cellulose membrane formed and fell off the plate glass. The cellulose membrane was left in deionized water for 24 h to dissolve out the excess NMMO. Afterward, the membrane was immersed into 30% glycerine solution to plastify for 0.5 h and air-dried at room temperature. A control membrane was prepared with the same method, without the addition of silver nitrate solution.

Morphological evaluation

Scanning electron microscopy (SEM) images were obtained on an S-4800 field emission scanning electron microscope (Rigaku, Japan) operated at 3.0 kV. All samples were sputtered with gold on an E-1030 ion sputtering equipment (Hitachi, Japan) before observation.

Structural characterization

X-ray diffraction (XRD) patterns of RC membranes were recorded on a D/max2200PC X-ray diffractometer (Rigaku, Japan) using Cu Kα radiation (λ = 0.154056 nm) operated at 40 kV.

The dried membranes were characterized using attenuated total reflectance Fourier transform infrared (ATR-FTIR) spectra from a VERTEX 70 (NETZSCH, Germany). The scanned area was in the range of 400 to 4000 cm^{-1} at a resolution of 4 cm^{-1}.

The dried membranes were also characterized *via* atomic force microscopy (AFM 5100, Agilent, USA) where a 2 μm × 2 μm view was observed.

UV–vis absorption spectra of RC membranes was recorded on a Cary 5000 UV–vis spectrophotometer with a scan range of 200 to 800 nm.

Silver content detection

A flame atomic absorption spectrometer (AAS) was used to detect the silver content of cellulose membranes. Additionally, 1 μg/mL, 2 μg/mL, 3 μg/mL, and 4 μg/mL silver standard solutions were used to draw a standard curve. The specimens were digested in 50% nitric acid solution before detection.

Antibacterial ability test

The antibacterial abilities of RC membranes against Gram-positive *S. aureus* and Gram-negative *E. coli* were tested by the agar diffusion method.

The recipe for the nutrient broth was as follows: 1 g of peptone, 0.5 g of beef extract, and 0.5 g of sodium chloride were dissolved in 100 mL of distilled water. The recipe for the agar medium was as follows: 1 g of peptone, 0.5 g of beef extract, 0.5 g of sodium chloride, and 1.5 g of agar powder were added to 100 mL of distilled water. The nutrient broth and agar medium both required sterilization before use. Bacteria were inoculated on agar medium plates for 24 h at 37 ± 2 °C. Afterward, typical bacterial colonies were selected for inoculation on 20 mL of nutrient broth at the same temperature. After 18 to 24 h, the nutrient broth, diluted twenty times, was used as an experimental bacteria suspension. Finally, circular and control specimens 15 ± 5 mm in diameter were prepared.

The liquid agar medium was poured into several petri dishes. After the agar medium had solidified, a bacteria suspension was uniformly coated on the surface of the agar medium. The specimens and controls were placed in the center of the plates and left for 18 to 24 h at 37 ± 2 °C. Afterward, the widths of the inhibition zones were calculated according to the following equation,

$$H = (D-d)/2 \tag{1}$$

where H is the bacteriostatic belt width, D is the average outside diameter of the inhibition zone, and d is the diameter of the specimen or control.

RESULTS AND DISCUSSION

Surface Plasmon Resonance of AgNPs

The AgNPs were roughly monitored by visual inspection of the RC membranes by color change (Hebeish *et al.* 2013; Prema *et al.* 2017).

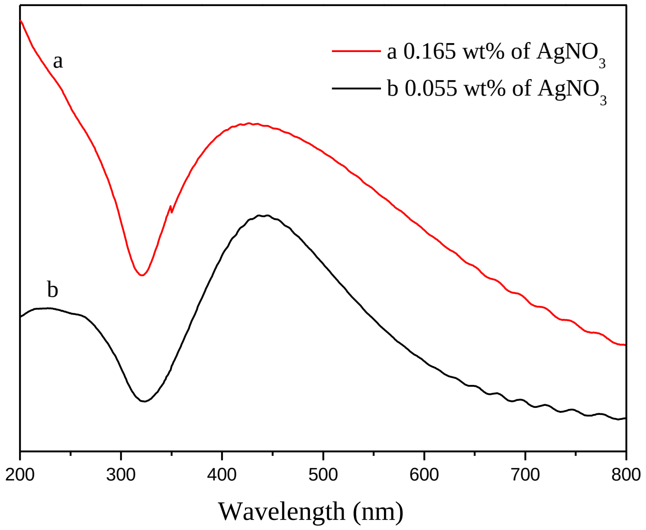

Fig. 1. UV–vis spectra of RC membranes loaded with (a) 0.165 wt% and (b) 0.055 wt% of $AgNO_3$

The AgNPs were roughly monitored by visual inspection of the RC membranes by color change (Hebeish *et al.* 2013; Prema *et al.* 2017). Preliminary characterization of the valence state of AgNPs was carried out using UV–vis spectrophotometer. Usually, AgNPs exhibit unique and tunable optical properties due to their surface plasmon resonance (Hebeish *et al.* 2010). The UV–vis spectra of RC membranes is shown in Fig. 1. As can be seen, a typical absorption spectrum at 430 nm was apparent for RC membranes, which was assigned to the surface plasmon resonance of AgNPs (Anderson *et al.* 2014). The result proved that elemental silver was in-situ synthesis on the RC membranes.

Morphology of RC Membranes

Scanning electron microscopy was employed to investigate the morphological characteristics of RC membranes, as well as the form and distribution of AgNPs on the membranes. As can be seen from Fig. 2, the structure of RC membranes was dense. AgNPs were distributed uniformly and were clearly visible as spherical particles on the surface of RC membranes. In this detection mode, AgNPs are highlighted because they have a higher atomic weight than the substrate (Barud *et al.* 2008). The illustration in Fig. 2b was particle size distribution, which was calculated by Nano Measurer. The particle size of AgNPs was in the range of 58 nm to 318 nm. The average particle size was 133 nm. Moreover, EDS was applied to confirm the existence of elemental silver.

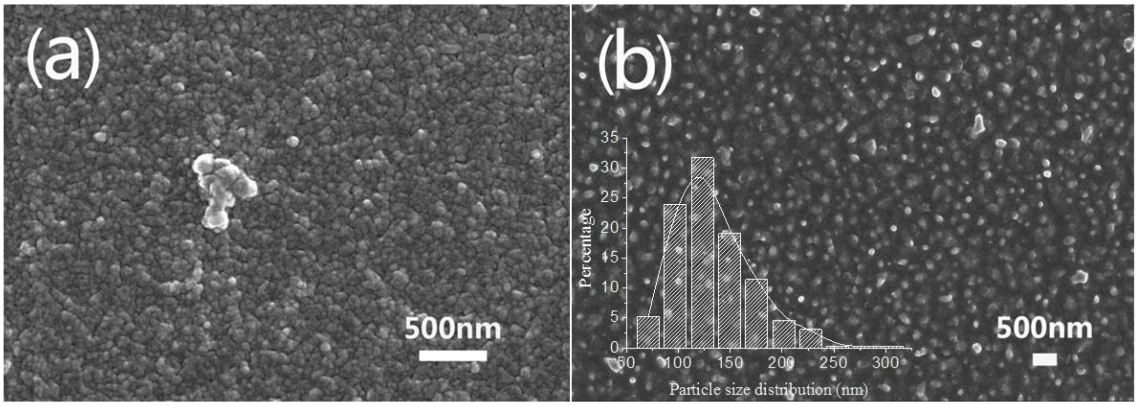

Fig. 2. SEM photographs of RC membranes loaded with (a) 0.055 wt% or (b) 0.110 wt% of $AgNO_3$

The EDS results showed that the specimens were composed of 1.11 wt% silver (Fig. 3). According to the results of SEM and EDS, it can be inferred that AgNPs were successfully loaded on RC membranes.

To obtain more information about the RC membranes, AFM was employed to observe the surface morphological characteristics. An AFM topographical image of the RC membrane surface is shown in Fig. 4. The inset shows the height parameters of the specimen. For better observation, the specimen here did not contain glycerin as a plasticizer. The morphology of the RC membrane showed a regular structure, which was caused by manual blade coating operation. The specimen exhibited high surface roughness, with a value of 7.19 nm shown in the inset. The value was higher than that gained *via* the spin coating method (3 to 4 nm) (Yokota *et al.* 2007). The spin coating method was carried out by machine, which is beneficial for industrial applications.

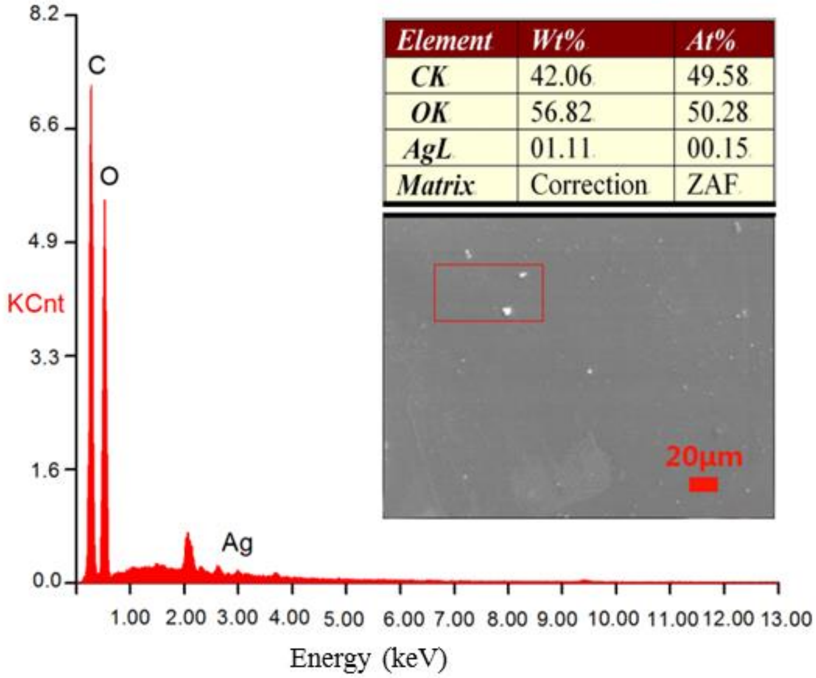

Element	*Wt%*	*At%*
CK	42.06	49.58
OK	56.82	50.28
AgL	01.11	00.15
Matrix	Correction	ZAF

Fig. 3. EDS analysis of RC membrane loaded with 0.110 wt% of $AgNO_3$

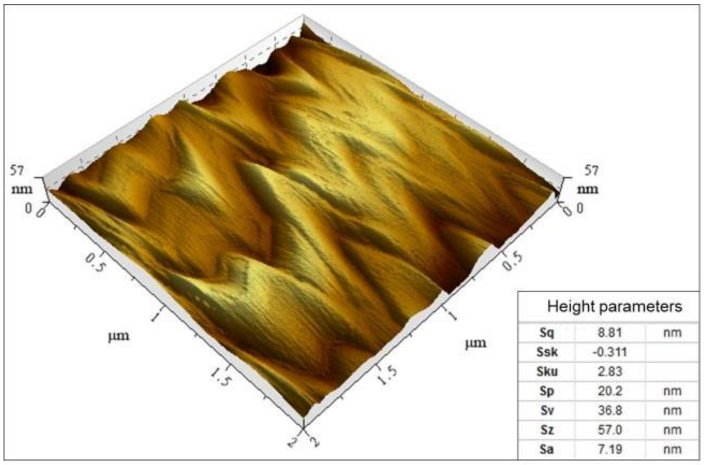

Height parameters		
Sq	8.81	nm
Ssk	-0.311	
Sku	2.83	
Sp	20.2	nm
Sv	36.8	nm
Sz	57.0	nm
Sa	7.19	nm

Fig. 4. AFM topographical image of RC membrane loaded with 0.165 wt% of $AgNO_3$

FTIR Analysis

FTIR spectra were used to characterize the structural changes of cellulose membranes after the addition of silver nitrate solution. As shown in Fig. 5, no new absorption peak appeared after the addition of the silver nitrate solution. This indicates that there were no obvious variations between the original cellulose and RC (Xu *et al.* 2015). To study the changes in the crystal lattice type of cellulose before and after regeneration, the FTIR spectra of cotton fibers and the RC membrane are shown in one plot for comparison (Fig. 6). Similar peaks for these two spectra can be observed. The band at 3317 cm^{-1} is due to OH- stretching. The peak at 2901 cm^{-1} corresponds to CH-stretching. The band at 1651 cm^{-1} is water -OH bending vibration. The absorption band at 1029 cm^{-1} is anti-symmetric stretching of the C–O–C bridge (Yin *et al.* 2006). On the contrary, dissimilarities at some frequencies can be found between these two spectra. As can be seen from the spectrum of the RC membrane (Fig. 6b), the band at 1417 cm^{-1} indicates that the RC membrane contained crystallized cellulose II (Nelson and O'Connor 1964a; Nelson and O'Connor 1964b). The bands at 1369, 1315, and 1157 cm^{-1} can be assigned to CH-stretching, CH_2 wagging, and C–O stretching in cellulose II, respectively (Široký *et al.* 2009). A small sharp band at 914 cm^{-1} represents the glycosidic C_1–H deformation with a ring vibration contribution, which is indicative of β-glycosidic linkages between sugar units. Moreover, the intensity of this band was somewhat higher compared with that of cellulose I (Carrillo *et al.* 2004), which corroborated the transition from cellulose I to cellulose II. Therefore, it can be concluded that the crystal lattice type of RC membranes changed from cellulose I to cellulose II without any derivatization during the dissolution and regeneration processes (Pang *et al.* 2013).

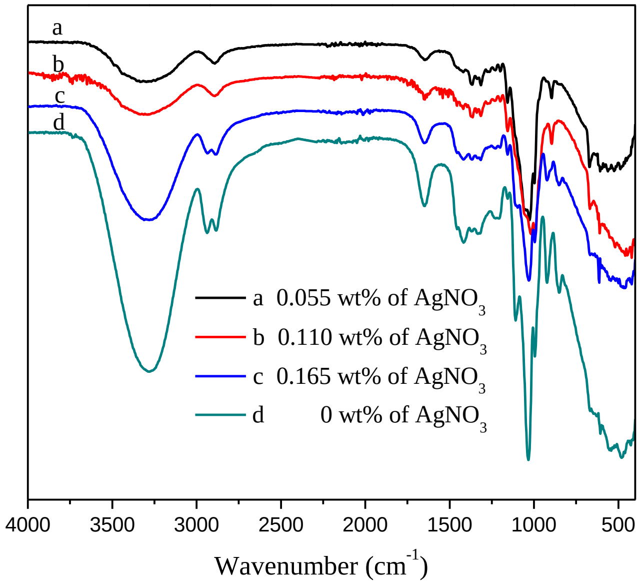

Fig. 5. FTIR spectra of cellulose membranes after the addition of silver nitrate solution

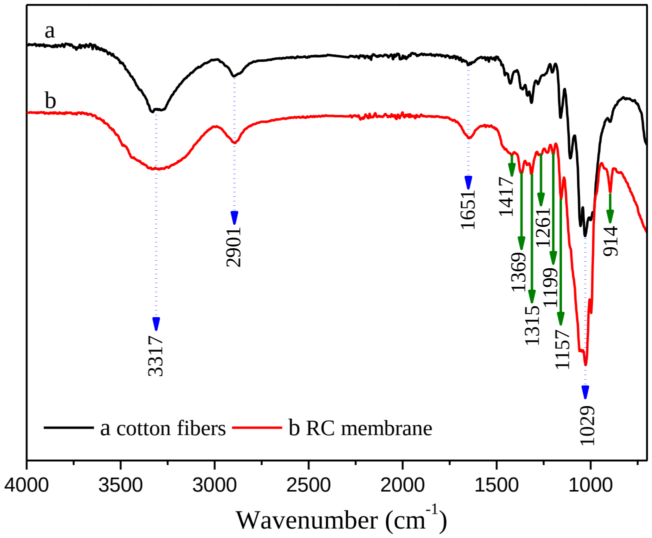

Fig. 6. FTIR spectra of cellulose (a) before and (b) after regeneration

X-Ray Diffraction

XRD was used to analyze the crystal lattice type of cellulose before and after regeneration. The X-ray patterns of cotton fibers and the RC membrane are shown in Fig. 7. As can be seen from the spectrum of cotton fibers (Fig. 7a), the strongest peaks were at 15.0°, 16.5°, 22.8°, and 34.4°, which corresponded to the 1-10, 110, 200, and 004 lattice planes of cellulose, respectively. Thus, the results indicate that the crystal structure of cotton fibers was cellulose I (Zhu *et al.* 2013). However, the strongest peaks of the RC membrane (Fig. 7b) were at 11.8°, 20.3°, and 21.7°, corresponding to the 1-10, 110, and 020 lattice planes of cellulose, respectively. The crystal structure of the RC membrane thus was determined to be cellulose II (Han and Yan 2010). Therefore, the XRD spectra indicate that the crystal structure of cellulose changed from cellulose I to cellulose II during the regeneration process, which is consistent with the FT-IR analysis.

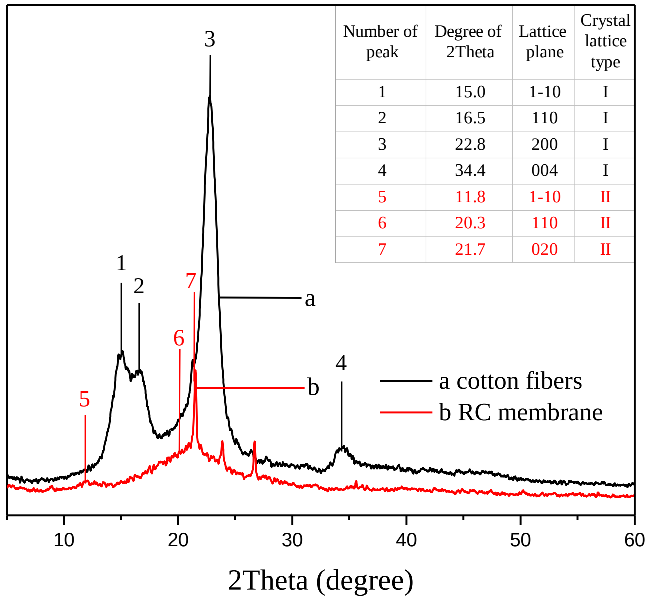

Number of peak	Degree of 2Theta	Lattice plane	Crystal lattice type
1	15.0	1-10	I
2	16.5	110	I
3	22.8	200	I
4	34.4	004	I
5	11.8	1-10	II
6	20.3	110	II
7	21.7	020	II

Fig. 7. XRD spectra of cellulose (a) before and (b) after regeneration

XRD was also used to determine the crystallinity changes in cellulose before and after regeneration. The results are shown in Table 1. The crystallinity decreased significantly during the dissolution and regeneration processes, from 63.57% for cotton fibers to less than 20% for RC membranes. The crystallization of NMMO during the molding of the cellulose/AgNPs/NMMO mixture may be the reason for the low crystallinity of the obtained RC membranes (El-Wakil and Hassan 2008).

Table 1. Crystallinity of Cotton Fibers and RC Membranes

Specimen	Silver nitrate percentage (wt%)	Crystallinity (%)
Cotton fibers	--	63.57
RC membranes	0	17.20
	0.055	11.71
	0.110	14.00
	0.165	11.14

Table 2. Silver Content and Bacteriostatic Belt Width of RC Membranes with Various Silver Nitrate Solution Loadings

Silver nitrate percentage (wt%)	Silver content (%)	H (mm)	
		S. aureus	*E. coli*
0.055	0.158	0.90	0.60
0.110	0.368	1.05	0.65
0.165	0.516	2.20	0.80

Antibacterial Ability of RC Membranes

Before characterizing the antibacterial ability, the silver contents of RC membranes were first determined *via* AAS. As can be seen from Table 2, the silver contents increased with increasing silver nitrate solution loading and reached the maximum value when the percentage of silver nitrate was 0.165 wt%. This indicates that the amount of AgNPs reduced by cellulose was gradually increased in this process.

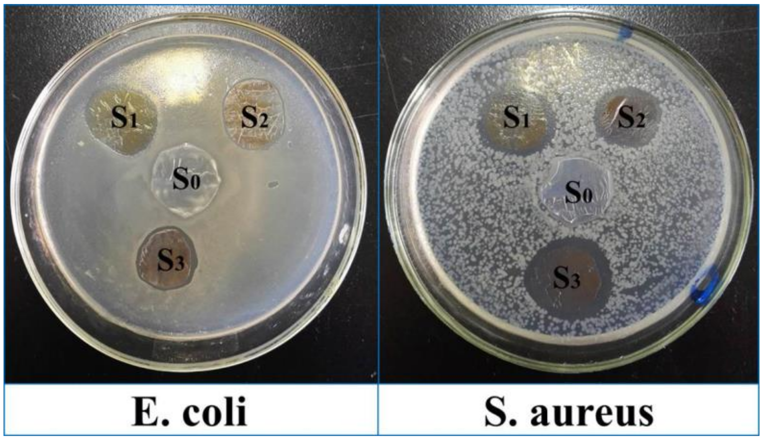

Fig. 8. Inhibition zones of RC membranes (S_0 is the control, and S_1, S_2, and S_3 are specimens loaded with 0.055 wt%, 0.110 wt%, and 0.165 wt% of silver nitrate, respectively)

S. aureus and *E. coli* were then employed as experimental cultures to determine the antibacterial ability of the specimens. It can be seen from Fig. 8 that there was no inhibition zone around the control specimens. This indicates that the control specimens did not have antibacterial properties.

Inhibition zones did appear around the silver-loaded RC membranes, which demonstrates that these specimens had antibacterial properties. The inhibition zones increased with increasing silver nitrate solution loading.

Combined with the silver content data in Table 2, it can be concluded that higher AgNP contents led to better antibacterial activities of RC membranes. With the highest AgNP content, S_3 exhibited the highest antibacterial properties, with respect to both *S. aureus* and *E. coli*, and the largest bacteriostatic belt width (data shown in Table 2). In addition, the antibacterial ability of silver-loaded RC membranes with respect to *S. aureus* was better than that against *E. coli*.

CONCLUSIONS

Antibacterial membranes loaded with silver nanoparticles (AgNPs) were presented, with regenerated cellulose (RC) as a matrix. Cellulose acted as a reducing agent, and silver nitrate acted as an oxidizing agent. The following conclusions were reached from this study:

1. AgNPs were reduced uniformly on RC membranes during the dissolution and regeneration of cellulose. The fabricated RC membranes exhibited high surface roughness, with a value of 7.19 nm.

2. The crystal lattice type of RC membranes changed from cellulose I to cellulose II, without any derivatization.
3. The silver contents increased with increasing silver nitrate solution concentration.
4. The silver-loaded RC membranes exhibited good antibacterial properties with respect to both *E. coli* and *S. aureus*.

ACKNOWLEDGMENTS

The authors are grateful for the support of the Open Fund of the State Key Laboratory of Pulp and Paper Engineering, South China University of Technology (201730), and the Shaanxi University of Science and Technology Academic Leader Training Program (2013XSD25).

REFERENCES CITED

Ahamed, M. I. N., Sankar, S., Kashif, P. M., Basha, S. K. H., and Sastry, T. P. (2015). "Evaluation of biomaterial containing regenerated cellulose and chitosan incorporated with silver nanoparticles," *International Journal of Biological Macromolecules* 72, 680-686. DOI: 10.1016/j.ijbiomac.2014.08.055

Anderson, R., Buscall, R., Eldridge, R., Mulvaney, P., and Scales, P. (2014). "Concentrated synthesis of metal nanoparticles in water," *RSC Advances* 4(60), 31914-31925. DOI: 10.1039/c4ra04223a

Barud, H. S., Barrios, C., Regiani, T., Marques, R. F. C., Verelst, M., Dexpert-Ghys, J., Messaddeq, Y., and Ribeiro, S. J. L. (2008). "Self-supported silver nanoparticles containing bacterial cellulose membranes," *Materials Science and Engineering: C* 28(4), 515-518. DOI: 10.1016/j.msec.2007.05.001

Carrillo, F., Colom, X., Suñol, J. J., and Saurina, J. (2004). "Structural FTIR analysis and thermal characterisation of Lyocell and viscose-type fibres," *European Polymer Journal* 40(9), 2229-2234. DOI: 10.1016/j.eurpolymj.2004.05.003

Castellano, J. J., Shafii, S. M., Ko, F., Donate, G., Wright, T. E., Mannari, R. J., Payne, W. G., Smith, D. J., and Robson, M. C. (2007). "Comparative evaluation of silver-containing antimicrobial dressings and drugs," *International Wound Journal* 4(2), 114-122. DOI: 10.1111/j.1742-481X.2007.00316.x

Chook, S. W., Chia, C. H., Zakaria, S., Ayob, M. K., Huang, N. M., Neoh, H. M., He, M., Zhang, L., and Jamal, R. (2014). "A graphene oxide facilitated a highly porous and effective antibacterial regenerated cellulose membrane containing stabilized silver nanoparticles," *Cellulose* 21(6), 4261-4270. DOI: 10.1007/s10570-014-0395-z

Dogan, H., and Hilmioglu, N. D. (2009). "Dissolution of cellulose with NMMO by microwave heating," *Carbohydrate Polymers* 75(1), 90-94. DOI: 10.1016/j.carbpol.2008.06.014

El-Wakil, N. A., and Hassan, M. L. (2008). "Structural changes of regenerated cellulose dissolved in FeTNa, NaOH/thiourea, and NMMO systems," *Journal of Applied Polymer Science* 109(5), 2862-2871. DOI: 10.1002/app.28351

Emam, H. E., and El-Bisi, M. K. (2014). "Merely Ag nanoparticles using different cellulose fibers as removable reductant," *Cellulose* 21, 4219-4230. DOI: 10.1007/s10570-014-0438-5

Emam, H. E., Ahmed, H. B., and Bechtold, T. (2017a). "In-situ deposition of Cu_2O micro-needles for biologically active textiles and their release properties," *Carbohydrate Polymers* 165, 255-265. DOI: 10.1016/j.carbpol.2017.02.044

Emam, H. E., El-Zawahry, M. M., and Ahmed, H. B. (2017b). "One-pot fabrication of AgNPs, AuNPs and Ag-Au nano-alloy using cellulosic solid support for catalytic reduction application," *Carbohydrate Polymers* 166, 1-13. DOI: 10.1016/j.carbpol.2017.02.091

Emam, H. E., El-Hawary, N. S., and Ahmed, H. B. (2017c). "Green technology for durable finishing of viscose fibers via self-formation of AuNPs," *International Journal of Biological Macromolecules* 96, 697-705. DOI: 10.1016/j.ijbiomac.2016.12.080

Feng, Q. L., Wu, J., Chen, G. Q., Cui, F. Z., Kim, T. N., and Kim, J. O. (2000). "A mechanistic study of the antibacterial effect of silver ions on *Escherichia coli* and *Staphylococcus aureus*," *Journal of Biomedical Materials Research Part A* 52(4), 662-668. DOI: 10.1002/1097-4636(20001215)52:43.0.CO;2-3

Fink, H. P., Weigel, P., Purz, H. J., and Ganster, J. (2001). "Structure formation of regenerated cellulose materials from NMMO-solutions," *Progress in Polymer Science* 26(9), 1473-1524. DOI: 10.1016/S0079-6700(01)00025-9

Han, D., and Yan, L. (2010). "Preparation of all-cellulose composite by selective dissolving of cellulose surface in PEG/NaOH aqueous solution," *Carbohydrate Polymers* 79(3), 614-619. DOI: 10.1016/j.carbpol.2009.09.008

Hebeish, A. A., El-RafieF, M. H., Abdel-Mohdy, F. A., Abdel-HalimH, E. S., and Emam, H. E. (2010). "Carboxymethyl cellulose for green synthesis and stabilization of silver nanoparticles," *Carbohydrate Polymers* 82(3), 933-941. DOI: 10.1016/j.carbpol.2010.06.020

Hebeish, A., Hashem, M., El-Hady, M. M., and Sharaf, S. (2013). "Development of CMC hydrogels loaded with silver nano-particles for medical applications," *Carbohydrate Polymers* 92(1), 407-413. DOI: 10.1016/j.carbpol.2012.08.094

Kowaluk, G. (2014). "Properties of lignocellulosic composites containing regenerated cellulose fibers," *BioRes.* 9(3), 5339-5348. DOI: 10.15376/biores.9.3.5339-5348

Luo, X., and Zhang, L. (2013). "New solvents and functional materials prepared from cellulose solutions in alkali/urea aqueous system," *Food Research International* 52(1), 387-400. DOI: 10.1016/j.foodres.2010.05.016

Morones, J. R., Elechiguerra, J. L., Camacho, A., Holt, K., Kouri, J. B., Ramírez, J. T., and Yacaman, M. J. (2005). "The bactericidal effect of silver nanoparticles," *Nanotechnology* 16(10), 2346-2353. DOI: 10.1088/0957-4484/16/10/059

Nelson, M. L., and O'Connor, R. T. (1964a). "Relation of certain infrared bands to cellulose crystallinity and crystal latticed type. Part I. Spectra of lattice types I, II, III and of amorphous cellulose," *Journal of Applied Polymer Science* 8(3), 1311-1324. DOI: 10.1002/app.1964.070080322

Nelson, M. L., and O'Connor, R. T. (1964b). "Relation of certain infrared bands to cellulose crystallinity and crystal lattice type. Part II. A new infrared ratio for estimation of crystallinity in celluloses I and II," *Journal of Applied Polymer Science* 8(3), 1325-1341. DOI: 10.1002/app.1964.070080323

Pang, J., Liu, X., Zhang, X., Wu, Y., and Sun, R. (2013). "Fabrication of cellulose film with enhanced mechanical properties in ionic liquid 1-allyl-3-methylimidaxolium chloride (AmimCl)," *Materials* 6(4), 1270-1284. DOI: 10.3390/ma6041270

Prema, P., Thangapandiyan, S., and Immanuel, G. (2017). "CMC stabilized nano silver synthesis, characterization and its antibacterial and synergistic effect with broad spectrum antibiotics," *Carbohydrate Polymers* 158, 141-148. DOI: 10.1016/j.carbpol.2016.11.083

Rai, M., Yadav, A., and Gade, A. (2009). "Silver nanoparticles as a new generation of antimicrobials," *Biotechnology Advances* 27(1), 76-83. DOI: 10.1016/j.biotechadv.2008.09.002

Simmons, T. J., Lee, S. H., Miao, J., Miyauchi, M., Park, T. J., Bale, S. S., Pangule, R., Bult, J., Martin, J. G., Dordick, J. S., *et al.* (2011). "Preparation of synthetic wood composites using ionic liquids," *Wood Science and Technology* 45(4), 719-733. DOI: 10.1007/s00226-010-0395-6

Široký, J., Blackburn, R. S., Bechtold, T., Taylor, J., and White, P. (2009). "Attenuated total reflectance Fourier-transform Infrared spectroscopy analysis of crystallinity changes in Lyocell following continuous treatment with sodium hydroxide," *Cellulose* 17(1), 103-115. DOI: 10.1007/s10570-009-9378-x

Wang, Q., Cai, J., and Zhang, L. (2014). "In situ synthesis of Ag_3PO_4/cellulose nanocomposites with photocatalytic activities under sunlight," *Cellulose* 21(5), 3371-3382. DOI: 10.1007/s10570-014-0340-1

Wong, K. K. Y., and Liu, X. (2010). "Silver nanoparticles-The real "silver bullet" in clinical medicine," *MedChemComm* 1(2), 125-131. DOI: 10.1039/C0MD00069H

Xu, Y., Zuo, L., Lin, T., Wang, J., and Yue, X. (2015). "Preparation and characterization of cellulose/Ag nanocomposites," *Polymer Composites* 36(12), 2220-2229. DOI: 10.1002/pc.23134

Yin, J., Luo, K., Chen, X., and Khutoryanskiy, V. V. (2006). "Miscibility studies of the blends of chitosan with some cellulose ethers," *Carbohydrate Polymers* 63(2), 238-244. DOI: 10.1016/j.carbpol.2005.08.041

Yokota, S., Kitaoka, T., and Wariishi, H. (2007). "Surface morphology of cellulose films prepared by spin coating on silicon oxide substrates pretreated with cationic polyelectrolyte," *Applied Surface Science* 253(9), 4208-4214. DOI: 10.1016/j.apsusc.2006.09.037

Zhu, Q., Zhou, X., Ma, J., and Liu, X. (2013). "Preparation and characterization of novel regenerated cellulose films *via* sol-gel technology," *Industrial and Engineering Chemistry Research* 52(50), 17900-17906. DOI: 10.1021/ie402791m

Article submitted: July 11, 2017; Peer review completed: September 4, 2017; Revised version received and accepted: October 9, 2017; Published: October 12, 2017.
DOI: 10.15376/biores.12.4.9050-9062